

## **Electrochemical and Spectroscopic Studies on Rated Capacitance and Aging Mechanisms of Supercapacitors**

P. KURZWEIL<sup>1</sup>, M. CHWISTEK

<sup>1)</sup> University of Applied Sciences, Kaiser-Wilhelm-Ring 23, D-92224 Amberg, p.kurzweil@fh-amberg-weiden.de

R. GALLAY<sup>2</sup>

<sup>2)</sup> Maxwell Technologies, CH-1728 Rossens, Switzerland

### **Abstract**

***ac* Impedance spectroscopy and transient techniques in different time domains were benchmarked for their benefit to determine rated capacitances of supercapacitors quickly and reliably, for example in industrial quality control. Scaling factors are presented to estimate rated *dc* capacitance by extrapolating 1 Hz *ac* capacitance: roughly 1.5 for acetonitrile systems, and 5 for propylencarbonate. A useful dimensionless number is introduced which allows to evaluate the quality of diverse production lots. Double-layer capacitors of different manufacturers were characterized in order to predict economic life-time and the statistical distribution of rated capacitance. Capacitance is shown as a dynamic quantity depending on voltage. Novel electrolyte systems based on ionic liquids are presented.**

*Keywords.* Double-layer capacitor aging and lifetime, rated capacitance determination, ionic liquids

### **1. Introduction**

The capacitance of so-called supercapacitors behaves somewhat mysterious in comparison with the well-known capacitance of the more or less ideal electronic components which have been in industrial use for more than a hundred years [1-3]. Capacitance reflects all the useful and parasitic chemical reactions at the phase boundary between the widely used active carbon electrodes and the organic electrolyte. The frequency response of capacitance does unfortunately not obey any simple series or parallel equivalent circuit of resistance and capacitance. In fact, capacitance must be understood qualitatively by help of the model for a porous electrode [4] and as a quantity strongly depending on voltage [5].

Industrial quality assurance during the fabrication of supercapacitors requires reliable and time-saving methods to determine rated capacitances. Based on our initial assumption that the numerical value of capacitance depends on the applied measurement techniques, we tried to gather the first

fundamental conversion factors for the comparison of *ac* impedance measurements [6] with transient techniques.

Furthermore we searched for fundamental insights into the properties and statistical distribution of capacitance in supercapacitors of different manufacturers.

In earlier long-time experiments [7], we studied the electrochemical decomposition of alkylammonium electrolytes in acetonitrile during the operation of supercapacitors. Therefore, exploring novel electrolytes, ionic liquids [8] were characterized by impedance spectroscopy for their use as stable substitutes of tetraethylammonium-tetrafluoroborate in acetonitrile. Future applications require electrolyte systems with high electrical conductivity and a broad voltage window far above 3.0 V.

## 2. Experimental

Our investigations try to answer the following questions:

1. How can rated capacitance be determined reliably and quickly?
2. Which conversion factors might be appropriate to compare directly capacitances determined by various electrochemical techniques working in different time domains?
3. How can be compared rated capacitances given by different manufacturers?

We investigated commercial capacitors of different manufacturers by *ac* impedance spectroscopy, cyclic voltammetry, and selected transient techniques.

*ac Impedance spectroscopy:* The fully discharged capacitors were characterized using a Solartron Frequency Response Analyser FRA 1250 and a standard resistor of 0.1  $\Omega$  in a frequency range between 10 kHz and 0.01 Hz. The excitation signal of 1 V was integrated over 30 cycles. A bias voltage was not applied.

*Cyclic voltammetry (CV):* The fully discharged capacitors were charged and discharged in the voltage range between zero and rated voltage (2.5 or 2.7 V) at a scan rate of 20 mV/s. The second cycle was used for capacitance determination.

*Transient techniques.* Constant-current discharge, and charge-discharge characteristics were recorded at fully discharged capacitors using a Solartron potentiostat SI 1287 and a power source (Gossen SSP 62 N) with a 0.1  $\Omega$  standard resistor of high quality (Burster), respectively.

*Ionic liquids* were characterized by impedance spectroscopy and cyclic voltammetry at room temperature in a measuring cell which consisted of two copper stamps in a fixed distance. Conductivity values were gauged by help of a potassium chloride solution.

### 3. Results and Discussion

#### 3.1 How capacitance depends on the measuring technique

Investigating commercial capacitors using *ac* impedance spectroscopy and transient techniques, we found the astonishing fact that the diverse time domains of measurement yield different results. **Figure 1** shows the capacitance values gathered by fast and slow measuring methods for a Maxwell 325 F supercapacitor. In detail:

a) Capacitance determined by *constant current discharge* characteristics strongly depends on the discharge current and the voltage (state of charge) of the capacitor. The simple method described in IEC 40/1378 [9] and applied in **Figure 2**, by which the linear drop from 80% to 40% of the rated voltage is evaluated, provides the highest capacitance values of all methods in the test. The supercapacitor is fully charged at its rated dc voltage for 24 hours. Then, the power source is cut off, and the capacitor is discharged by help of an electronic load at a moderate constant current of about 5 mA/F. Capacitance and equivalent series resistance are given by:

$$C = \frac{I \cdot (t_2 - t_1)}{U_1 - U_2}, \quad \text{and} \quad R = \frac{\Delta U_R}{I} \quad (1)$$

$t_2 - t_1$  equals the period of time during which the voltage across the capacitor declines from 80% to 40% of the applied voltage  $U_0$ . The ohmic voltage drop  $\Delta U_R$  is determined as the point of intersection between the linearly extrapolated voltage curve and the time axis immediately after closing the discharge circuit ( $t_0$ ).

At higher currents, the linear voltage region in the discharge characteristics becomes too narrow (see Figure 2a), and the error of the capacitance calculated by  $C = I \cdot \Delta t / \Delta U$  increases dramatically. Evidently, capacitance strongly depends on the voltage window which is passed during discharge.

b) *Integration method*. Exact measurements following the definition of capacitance,  $C = Q/U$ , therefore require to integrate the current flowing through the supercapacitor with respect to time. The correction of leakage currents  $I(t \rightarrow \infty)$  may be neglected in most cases. The higher the discharge current, the higher is the calculated capacitance  $C$ , which reaches a constant value after some minutes of discharge time  $t$  (see **Figure 2b**).

$$C = \frac{1}{U_0 - U(t)} \int_0^t I(t') dt' \quad (2)$$

At operating voltages lower than the rated voltage  $U_0$ , smaller capacitance values are measured, because the capacitor has not reached its full state-of-charge. In the electric field at 2.5 V a higher capacitance is observed than at 1 V or 1.5 V. Indeed, capacitance shows the linear dependence on voltage  $C(U) = C_0 + \text{const} \cdot U$ , which is outlined in section 3.2. The discharge method captures capacitance at a certain state-of-charge given by the *dc* charging conditions – i. e. capacitance comprises both the fast discharge process at the “outer” double-layer capacitance of the electrode/electrolyte interface and the “inner” pseudo-capacitance of the slow, diffusion controlled faradaic reactions in the electrode pores (see **Figure 3**).

c) *Chronoamperometry*, the current response after a voltage step, allows to determine the rated capacitance of supercapacitors in industrial quality control within a few seconds. Before the measurement, the capacitor terminations are short-circuited for at least 30 minutes. With switching on the power source at the point of time  $t = 0$ , the applied voltage jumps from 0 V to  $U_0 = 2,5$  V. A current peak occurs, followed by an approximately linear decrease of current  $dI/dt$  within about 3 seconds (for a 350 F capacitor). At longer times, the charge curve shows an exponential decay. The current response – measured as voltage drop across a shunt – is recorded using an oscilloscope.

$$C = -\frac{U_0}{R_1^2 \left. \frac{dI}{dt} \right|_{t=0}} \quad \text{and} \quad R_1 = \frac{U_0}{I(t=0)} \quad (3)$$

$R_1$ , sum of standard resistor (e.g. 0.02  $\Omega$ ), contact resistances, and series resistance of the capacitor. As the total current flows across  $C$  at the beginning of charging ( $t \rightarrow 0$ ), all slow electrode reactions can be neglected. As a result, the value of capacitance calculated from the applied voltage  $U_0$  and the initial slope of current is considerably smaller than the value found by the constant current discharge method. With reference to the Figures 1 and 3, we state that the current response method reflects the rapid electrode reactions at the “outer” double-layer capacitance  $C_0$  of the uncharged capacitor without the slow faradic reactions controlled by pore diffusion.

d) *ac impedance spectroscopy* and *cyclic voltammetry* provide differential capacitances which depend on voltage, frequency and scan rate, respectively. The integral average value – or the differential capacitance at 50% of the rated voltage – may be considered as most accurate and reliable values for the rated capacitance of a commercial supercapacitor (see section 3.3). Figure 1 shows that *ac* impedance spectroscopy yields the value  $C_0$ , if no bias is applied, whereas cyclic voltammetry regards the voltage dependent capacitance  $C(U)$  outlined in section 2.3.

e) *Pseudocapacitance*. The molecules at the electrochemical interface between electrode and electrolyte show a nonlinear response to the electric field. Capacitive and Faradaic charges coexist. This charge, divided by the potential range from which it is transferred, constitutes a pseudocapacitance since it is not associated with a purely capacitive phenomenon [3].

Transient techniques, which generate fast voltage changes, reflect the fast charge/discharge processes with “frozen” diffusion at the outer electrode surface. At slow voltage changes the slow electrode reactions in the inner electrode surface (strongly depending on voltage) additionally contribute to the measured capacitance values.

We conceive capacitance as a dynamic quantity, that depends on the voltage and the state of charge of the supercapacitor. Capacitance may be divided up in a double-layer capacitance at the “outer” electrode surface and a pseudo-capacitance due to slow electrochemical processes depending on voltage (see **Figure 3**). The linear voltage dependence of capacitance is outlined in the following.

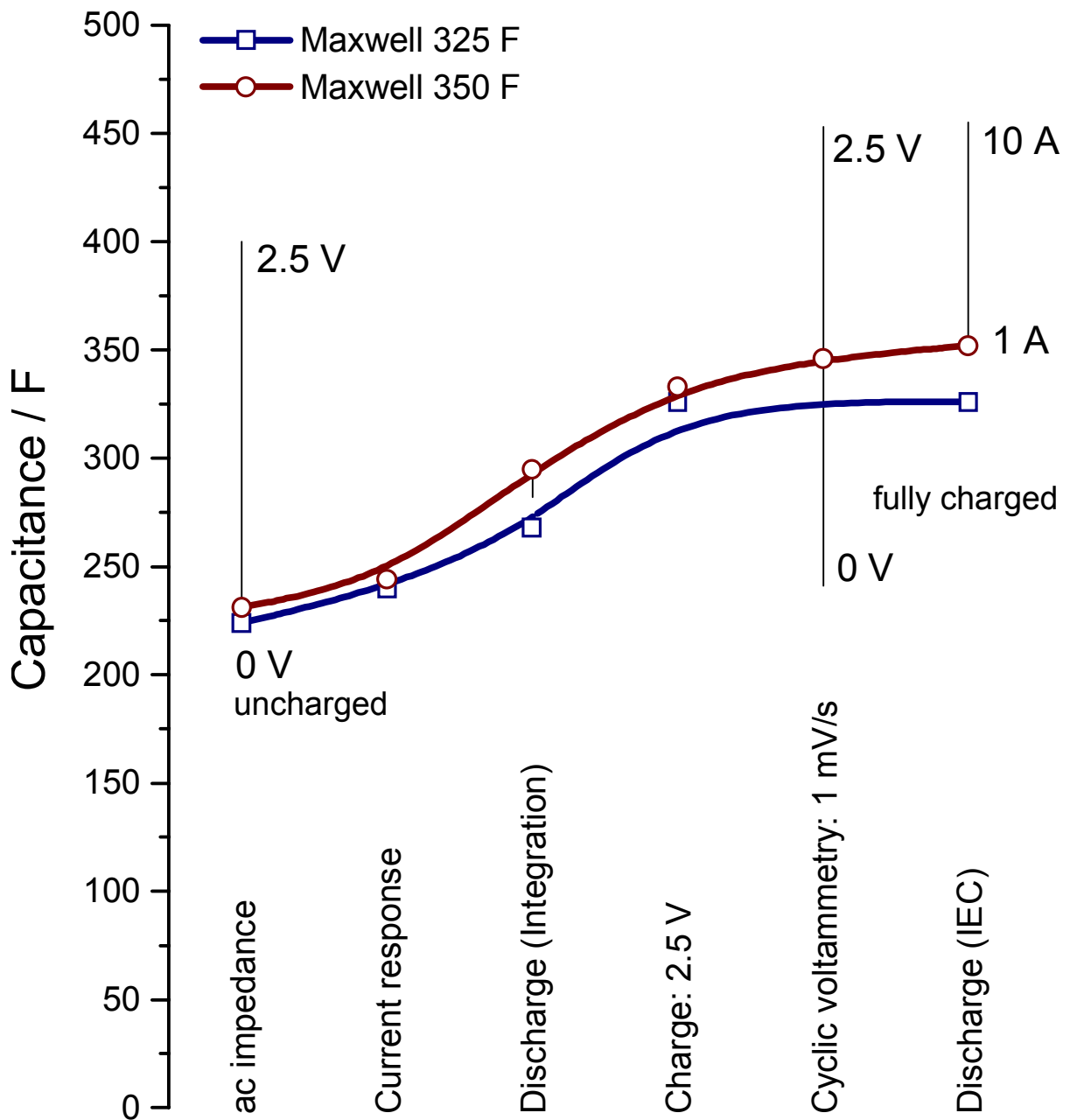
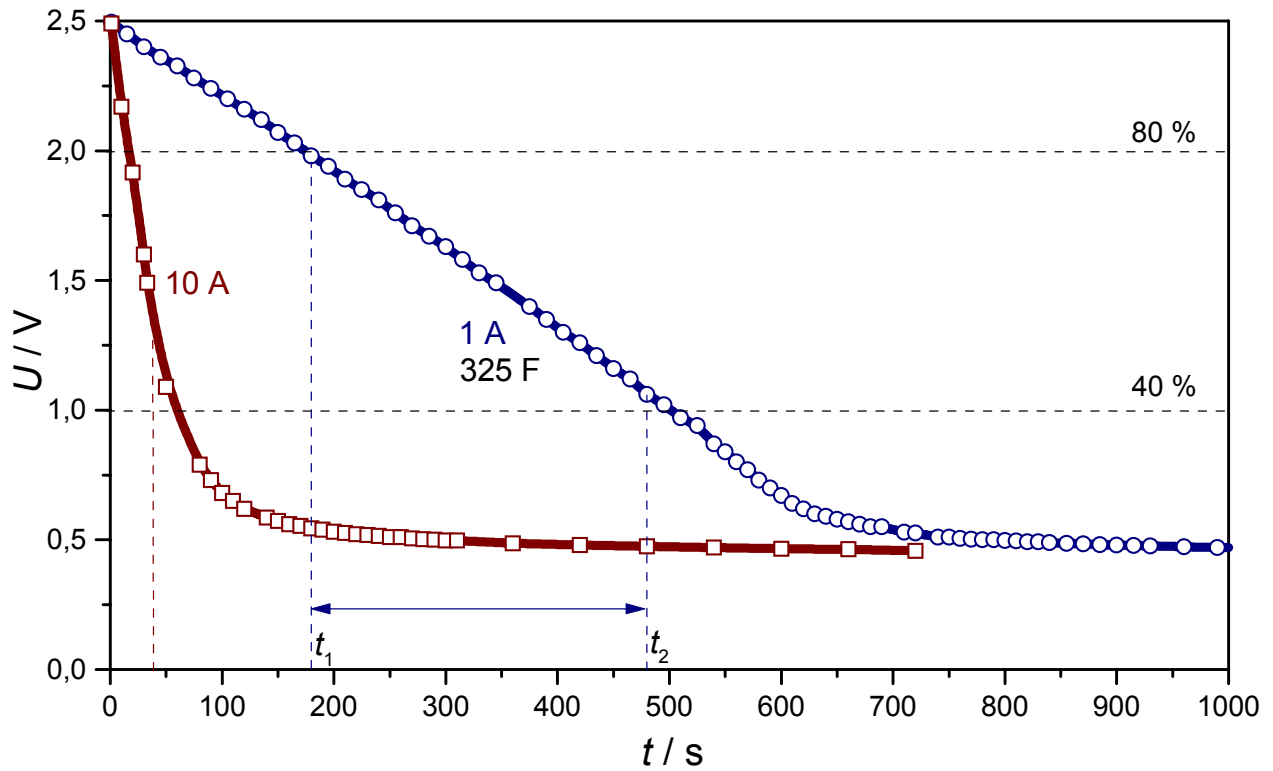
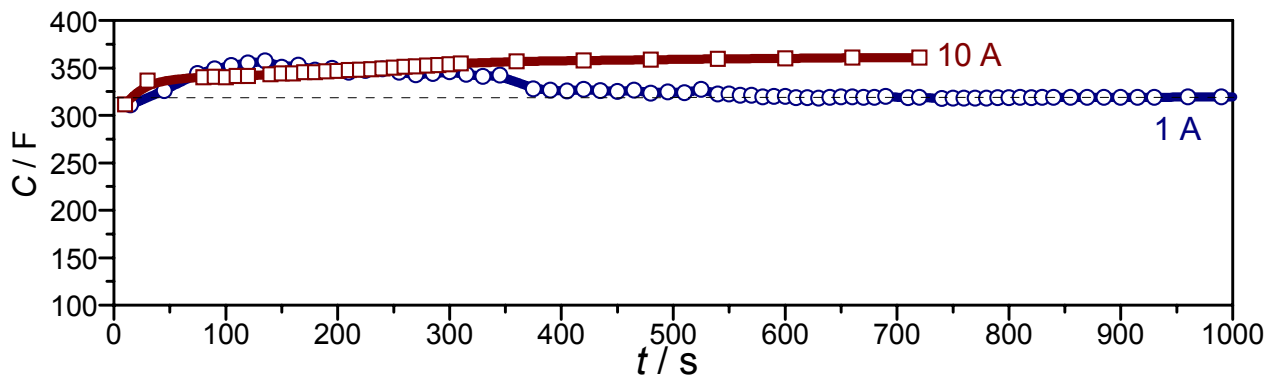
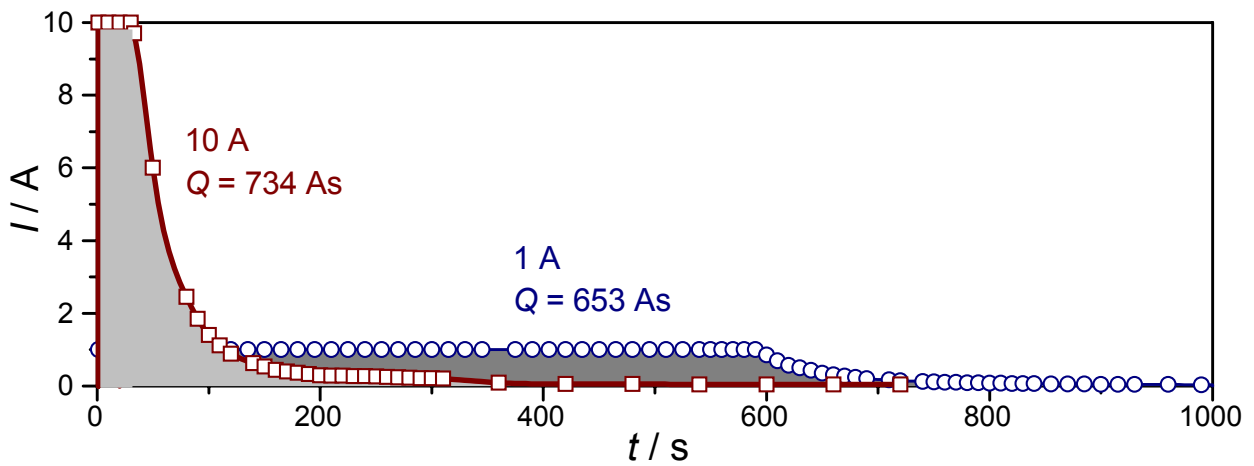


**Fig. 1: Capacitance of Maxwell capacitors (BCAP0350) determined by different techniques, which cause a different state-of-charge of the capacitor.**

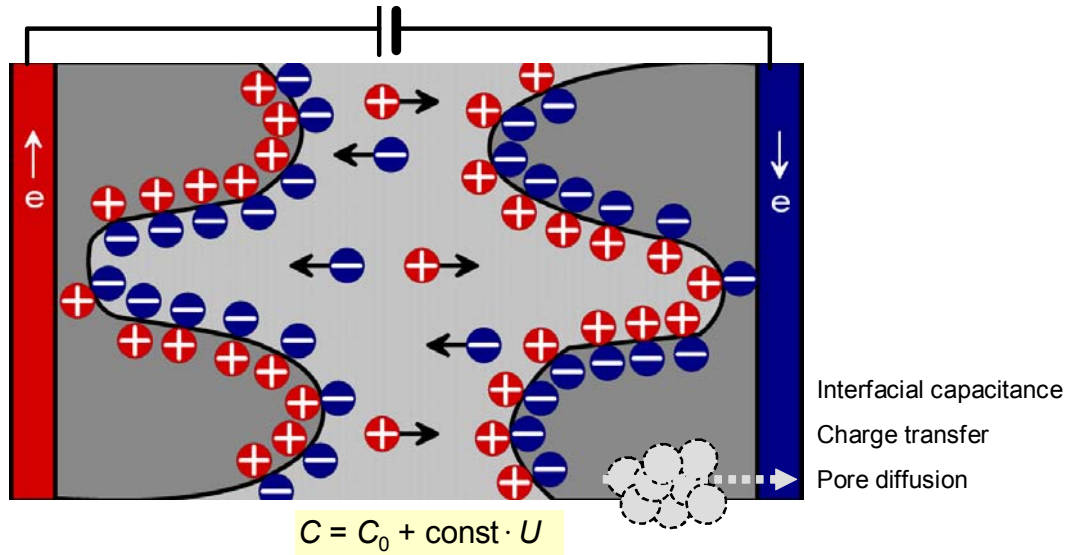


a)



b)

**Fig. 2: Determination of capacitance using a constant current discharge according to a) IEC 40/1378 and b) the integration method (see text). Maxwell "BCAP0350" supercapacitors (325 F/2.5 V) at different discharge currents of 1 A and 10 A.**



**Surface capacitance**  
 Charge of *outer electrode surface*  
 at fast change of voltage (high frequency)

**Bulk capacitance and electrokinetics**  
 Charge of *inner electrode surface*  
 at slow change of voltage (low frequency)

**Fig. 3: Model for the capacitance of a supercapacitor due to the double-layer  $C_0$  and faradic reactions  $C(U)$ .**

### 3.2 Capacitance: a linear function of voltage

Capacitance and electric charge of supercapacitors depend on the applied voltage, as we learnt on a spring morning in 1997 [10], when we started a Mercedes C220 by a 30 V/65 F bipolar supercapacitor at an ambient temperature of 12 °C. The battery was completely disconnected from the starter. The transients of capacitor current and voltage were recorded during cranking by help of an oscilloscope. A single start required an almost constant electric power of 1 kW, an electric charge of 150 As and a minimum capacitance of 33 F. Voltage dropped to 4.5 V depending on the operating voltage of the starter (12–18 V).

The transients during constant current discharge are shown in **Figure 4**. Capacitance was determined according to equation (1). At constant discharge currents between 10 and 100 A, we observed that capacitance and electric charge depend linearly on the applied voltage.

$$C(U) = \frac{Q(U)}{U} \approx 60 \text{ F} + 0.14 \text{ F} \cdot U \quad (4)$$

Capacitance seems to be an approximately linear function of voltage:  $C(U) = C_0 + k \cdot U$ , whereby  $C_0$  is the capacitance at 0 V.

Understanding  $C(U)$  as a linear function of voltage, we get corresponding expressions for current, capacitance and energy [5,11,12]:

$$I = \frac{dQ}{dt} = \frac{d(C(U)U)}{dt} = \frac{d([C_0+kU]U)}{dt} = (C_0+2kU) \frac{dU}{dt} \quad (5a)$$

$$C(U) = \frac{Q}{\Delta U} = \frac{1}{\Delta U} \int_0^{\Delta U} (C_0 + 2kU) dU = C_0 + k \Delta U \quad (5b)$$

$$W = \int_0^{\Delta U} U(t) \cdot I(t) dt = \int U dQ = \int U d[C(U)U] = \int U(C_0 + 2kU) dU = \frac{1}{2} C_0 U^2 + \frac{2}{3} k U^3 \quad (5c)$$

The notion of capacitance is well understood when it is constant in the voltage domain. In the case of a voltage linear dependency, a clear difference must be done between the  $C$ -coefficient in the relation linking the current amplitude  $I(t)$  and the voltage change  $dU/dt$  and the  $C$ -coefficient linking the charge and the voltage. What we are used to call the capacitance is in the constant case the  $C$ -coefficient which is equal for both relations. This insight is verified in the following.



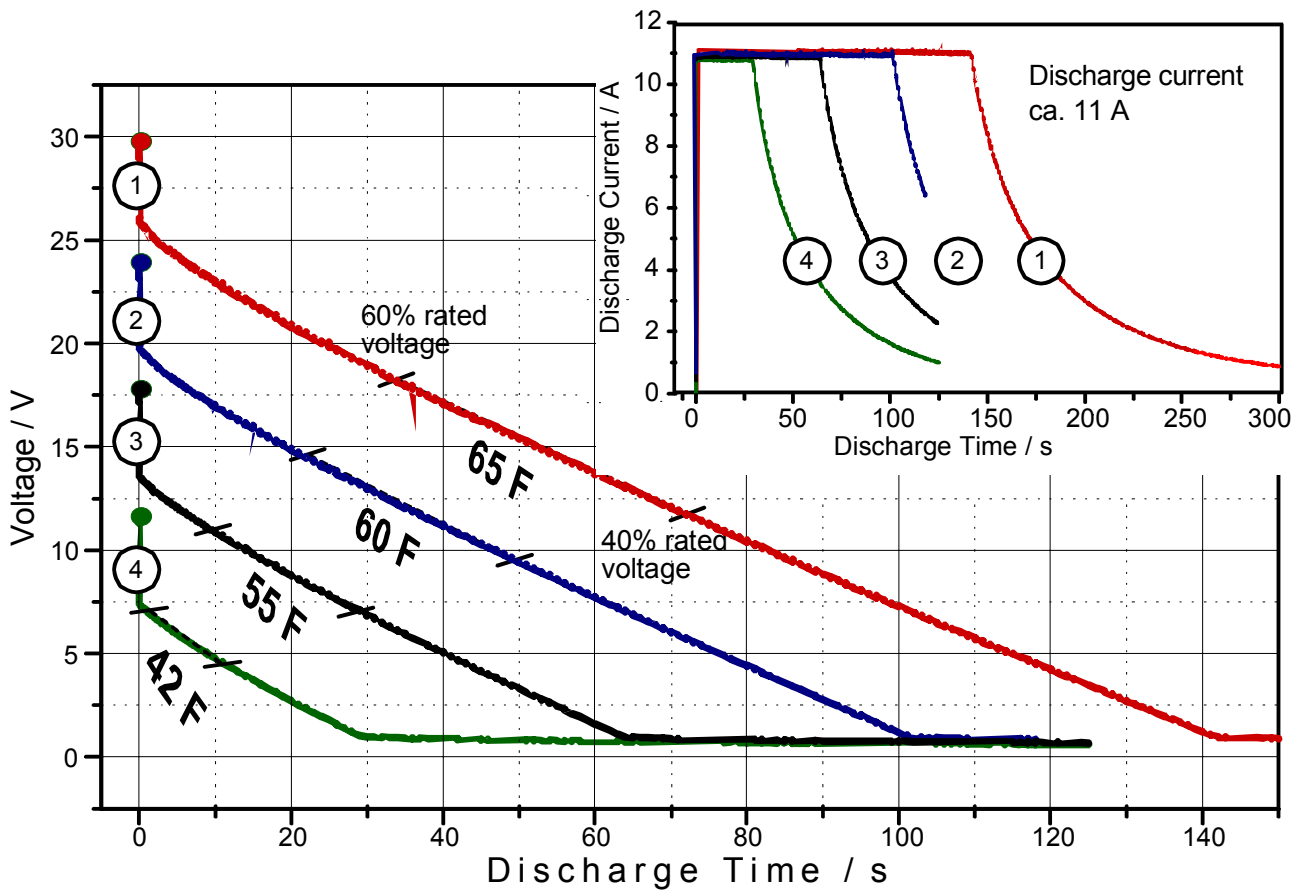


Fig. 4: Constant current discharge characteristics of a 30 V/65 F bipolar supercapacitor at different operating voltages  $U$  (states of charge). Capacitance was determined by  $C = I \cdot dU/dt$  at a discharge current of  $I = 11$  A.

### 3.3 Rated capacitance determination by cyclic voltammetry

The linear dependence of capacitance on voltage  $C(U) = C_0 + k \cdot U$  can be understood by help of the cyclic voltammogram. A supercapacitor may have a differential capacitance  $dQ/dU$  (at a certain voltage), with a corresponding medium integral capacitance  $Q/\Delta U$  (in a certain voltage window). By help of electric charge  $Q$ , we are able to describe the pseudocapacitance of a supercapacitor as a differential quantity which depends on the scan rate  $\nu$  of voltage.

$$Q = \int_0^{\Delta t} I(t) dt = \frac{1}{\nu} \int_0^{\Delta U} I(U) dU \quad \text{and} \quad \nu = \frac{dU}{dt} \quad (6a)$$

Integral capacitance equals the average value of differential capacitance. It can directly be read from the cyclic voltammogram at 50% of the rated voltage as shown in **Figure 6**.

$$\bar{C} = \frac{Q}{\Delta U} = \frac{1}{\Delta U} \int_0^{\Delta U} C(U) \cdot dU = C(U_0/2) \quad (6b)$$

Differential capacitance, at a constant scan rate  $\nu$ , is directly depending on the flowing current.

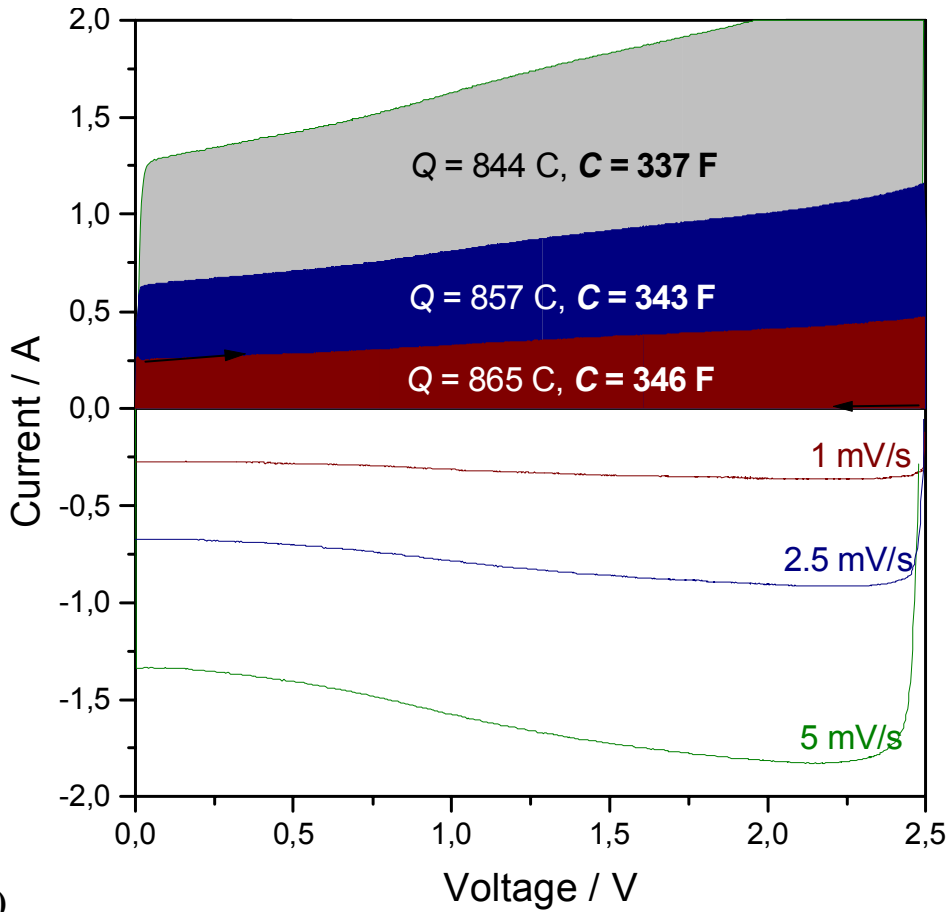
$$C(U) = \frac{dQ}{dU} = \frac{I(U)}{\nu} \quad \text{and} \quad I = \frac{dQ}{dt} = C \frac{dU}{dt} = C\nu \quad (7a)$$

As the charge and discharge cycle are not identical, due to irreversible processes and the internal resistance of the supercapacitor, the average value of charge and discharge current,  $I_c$  and  $I_d$ , may be calculated advantageously. Finally, capacitance determination is enormously simplified by separately averaging both all the current values in the charge cycle and in the discharge cycle and averaging them.

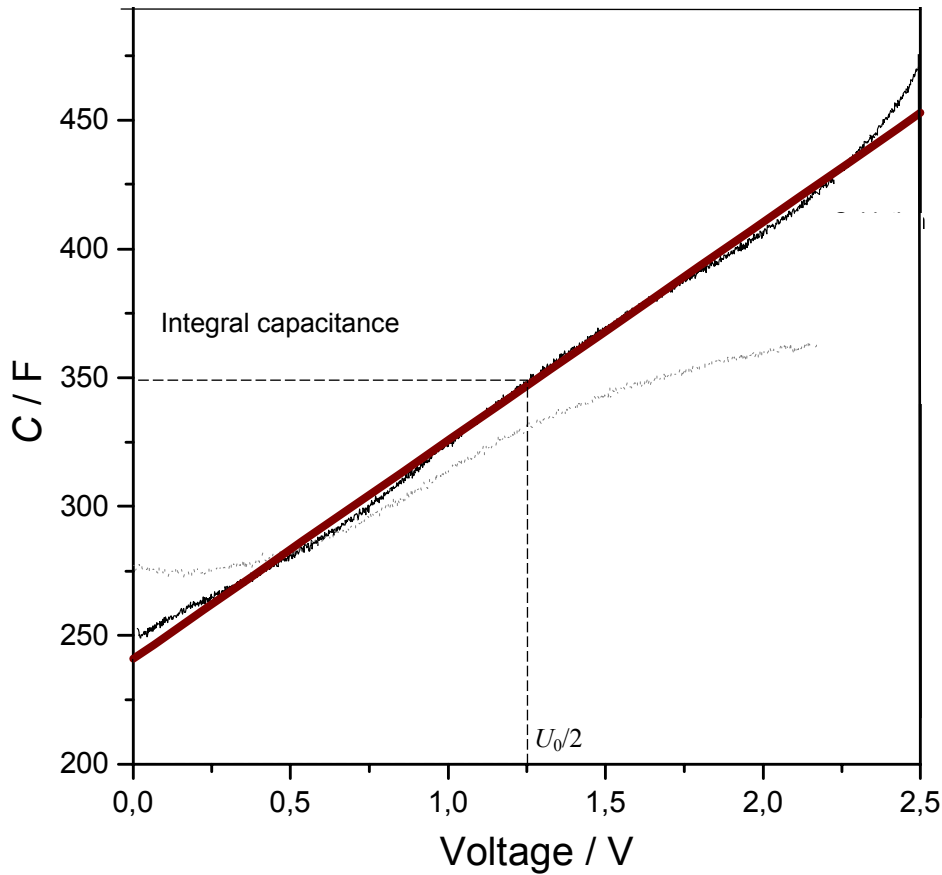
$$C = \frac{\bar{I}_c + \bar{I}_d}{2\nu} \quad (7b)$$

We proved by measurements at serveral hundered capacitors (not shown here) that equation (7b) provides nearby the same results than averaging the exact values by integration of the charge and discharge cycle (equation 6b). The error is the third significant digit.

With reference to Figure 3, the scan rate  $\nu$  must be low to record *dc* capacitance caused by slow electrode processes in the “inner” surface of the electrode pores.



a)



b)

**Fig. 5: Detemination of rated capacitance of a MAXWELL supercapacitor (350 F, 2.5 V) by cyclic voltammetry at different scan rates: a) by the integration method, b) by averaging of differential capacitance  $C(U) = 241 \text{ F} + 85 \text{ U/V}$  at a scan rate of 1 mV/s (fit quality 99,8%).**

### 3.4 Quality control by cyclic voltammetry

The statistical distribution of the rated capacitances in four random samples of 50 supercapacitors was tested to prove cyclic voltammetry as an appropriate method. According to equation (7b), capacitance was determined by averaging the current values of the charge cycle and the discharge cycle. The results are shown **Table 1**. Some manufacturers provide more capacitance than is printed on the capacitor case, other manufacturers provide less.

We recommend cyclic voltammetry as a most precise, robust and uncorruptible method to determine rated capacitances. More or less vague estimations of voltage drops, as required by the IEC current discharge method, are not necessary. Unfortunately, CV requires a long measuring time of about nine to 18 minutes per sample to guarantee quasistationary conditions at low scan rates of 0.01 to 0.02 V/s. The second cycle could be evaluated reasonably, because the first cycle is typically distorted by residual charges in the capacitor. Nevertheless, we were able to evaluate the first cycle according to equation (7b), even though charge wave and discharge wave were not perfectly symmetrical, and a slightly increased error of capacitance had to be tolerated.

Therefore, the speed of *ac* impedance spectroscopy should be combined with the advantages of cyclic voltammetry as outlined in the following.

**Table 1: Rated values of capacitance and series resistance determined by cyclic voltammetry and impedance spectroscopy. The given error equals the experimental standard deviation.**

Rated value	Manufacturer A Carbon/acetonitrile		Manufacturer B Carbon/propylen carbonate	
	a) 50 F	b) 100 F	a) 50 F	b) 100 F
a) Cyclic voltammetry				
Capacitance at 0.02 V/s <sup>a</sup>	51 ± 1.7 F	112 ± 1.8 F	41 ± 0.7	80 ± 0.8 F
b) <i>ac</i> -impedance spectroscopy:				
Capacitance at 0.01 Hz	50	110	34	66
Capacitance at 1 Hz <sup>b</sup>	33.7 ± 2.3 F	65.0 ± 8.2 F	7.14 ± 0.56	14.7 ± 0.54
Scaling factor $C_{0.01\text{Hz}}/C_{1\text{Hz}}$	1.5	1.7	4.8	4.5
Scaling factor $C_{\text{CV}}/C_{1\text{Hz}}$	1.5	1.7	5.7	5.4
Resistance at 100 Hz <sup>b</sup>	14.8 ± 1.2 mΩ	13.0 ± 2.2 mΩ	31.2 ± 2.0 mΩ	22.2 ± 6.5 mΩ

<sup>a</sup> average of 50 capacitors, <sup>b</sup> average of 600 capacitors

### 3.5 Scaling factors for ac impedance spectroscopy

The frequency response of capacitance strongly depends on frequency as shown in **Figure 6**. Constant current discharge and cyclic voltammetry at slow scan rates provide *dc* values of capacitance. *ac* Impedance spectroscopy provides such values even at relatively long measuring times. We found that commercial capacitors rated at 10 F require a minimum frequency below 0.5 Hz, capacitors rated at 100 F below 0.05 Hz, capacitors rated at 1000 F and more below 0.01 Hz. Our approach is therefore to extrapolate to the wanted *dc* values from *ac* capacitances gathered at high-frequency.

Figure 6 shows the frequency response of capacitance of commercial supercapacitors in the frequency range between 1 kHz and 0.01 Hz. A bias voltage was not applied. Capacitance was calculated by help of the imaginary part of complex impedance regarding a simple R-C series network.

$$C(f) = \frac{-1}{2\pi f \cdot \text{Im } \underline{Z}} \quad (8)$$

The frequency response reveals a fundamental difference between the capacitors based on different electrode structures and electrolyte systems (acetonitrile and propylencarbonate respectively).

The A type capacitors provide capacitive behaviour below 100 Hz, above 100 Hz they behave inductively. The rated capacitance printed on the capacitor cases of 50 and 100 F respectively is reached in the frequency range between 0.1 and 0.01 Hz. 80% of the rated capacitance are available at 1 Hz.

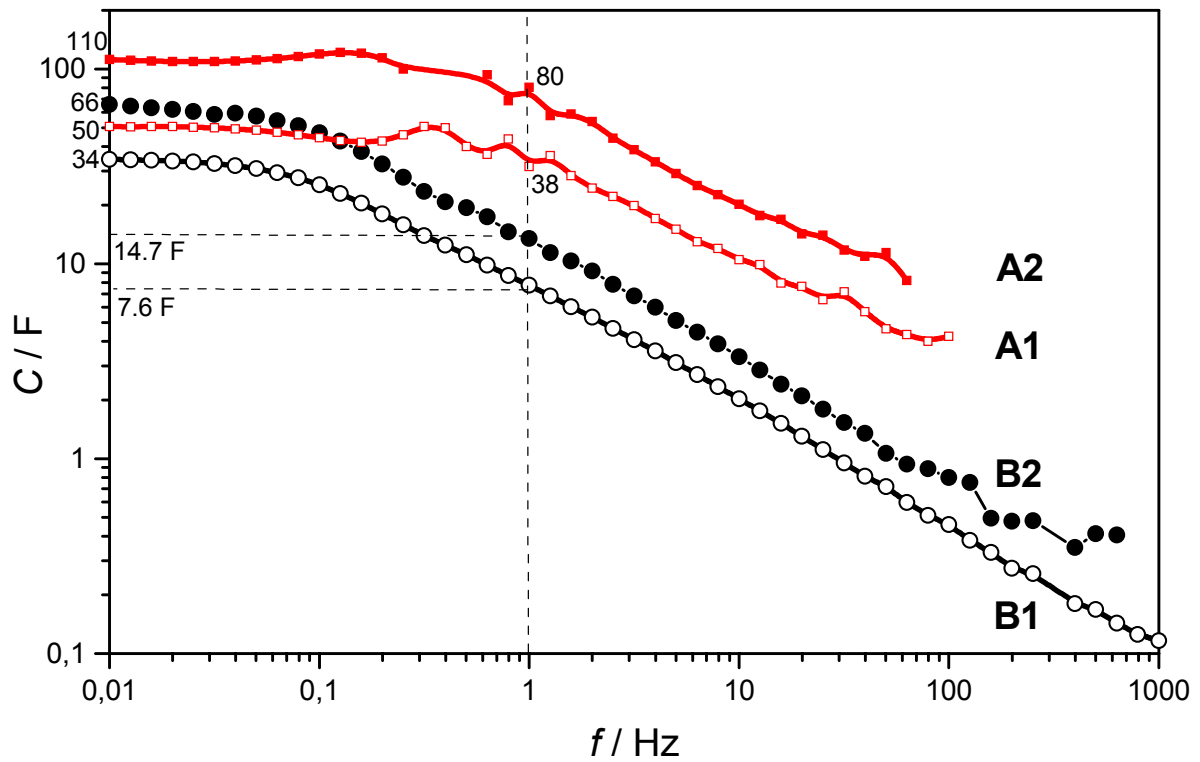
The B type capacitors fail above 500 to 1000 Hz. The rated capacitance printed on the cases are too high. Even at 0.01 Hz rated capacitance is not available. 20% of the rated capacitance is available at 1 Hz.

We verified the following statistical evaluation procedure in order to compare diverse lots of supercapacitors stemming from different manufacturers:

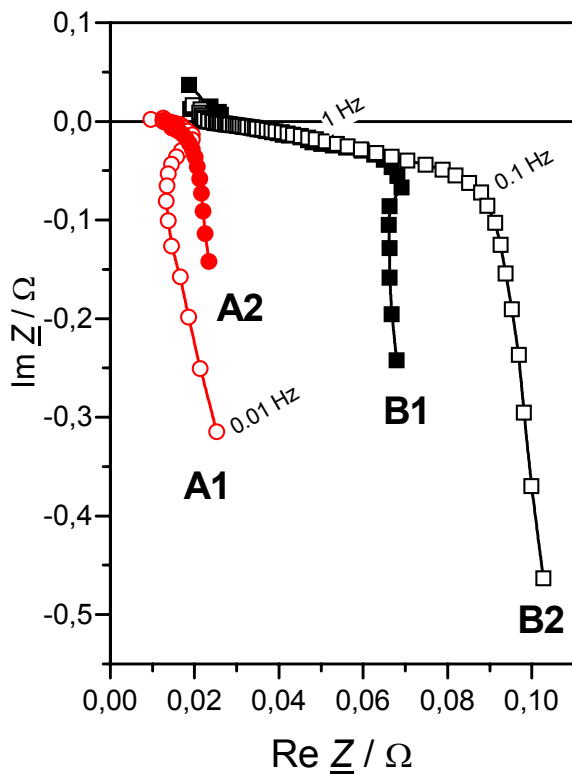
1. Determination of true rated *dc* capacitance by cyclic voltammetry at a slow scan rate using a representative lot of 20 to 50 capacitors. Alternatively, impedance spectroscopy in the frequency range down to 0.01 Hz can be employed.
2. Fast *ac* impedance measurements allow to gather series resistance at 100 Hz and capacitance at 1 Hz for a statistical lot of several hundreded capacitors within reasonable time (about 30 seconds per capacitor). Rated *dc* capacitance is extrapolated by multiplying the 1 Hz capacitance with the scaling factor *f* according to equation (9).

$$C_{dc} = f \cdot C_{1\text{Hz}} = \begin{cases} 1.5 \cdot C_{1\text{Hz}} & \text{(acetonitrile)} \\ 5 \cdot C_{1\text{Hz}} & \text{(propylencarbonate)} \end{cases} \quad (9)$$

As shown in the example in **Table 1**, the scaling factor depends primarily on the electrode/electrolyt system. Size and geometry of the capacitor play a secondary role. The scaling factor is obtained by dividing the average value of *dc* capacitance by the average value of *ac* capacitance at 1 Hz, whereby a representative lot of supercapacitors is considered. Afterwards, fast *ac* impedance measurements according to equation (9) are useful for time-saving quality control of even huge numbers of supercapacitors.



a)



b)

**Fig. 6: Frequency response of capacitance (a) and complex plane plot (b) of supercapacitors of two manufacturers (A, B) rated at 1 = 50 F, and 2 = 100 F.**

### 3.6 A novel quality criterion

In order to simplify the choice of supercapacitors appropriate to a certain technical application, the rated data may be compared by help of the following dimensionless quantity.

$$g = \frac{C_1}{R_{100}} \cdot \frac{R_n}{C_n} \gg 1 \quad (10)$$

Herein,

- $C_1$  measured series *ac* capacitance at 1 Hz
- $R_{100}$  measured series resistance at 100 Hz
- $R_n$  rated resistance, average of the  $R_{100}$ -values of all capacitors in the test
- $C_n$  rated capacitance as printed on the capacitor case (or average value of dc capacitance measured by slow cyclic voltammetry).

The quantity  $g$  gets a big value for capacitors with high capacitance and slow resistance. With reference to the rated data or the average values of all capacitances and resistances in the test, the  $g$  value are distributed around 1.

The example in **Figure 7** shows the quantity  $g$  for four lots of 600 supercapacitors in each case. The horizontal line  $g = 1$  marks the “average quality”. The ten percent of the best capacitors lie clearly above 1, and the ten percent of the worst samples lie below 1. The A2 type capacitors really provide the highest capacitance and the lowest resistance useful for the technical application, although the B2 type was designated with the identical rated values by a different manufacturer.

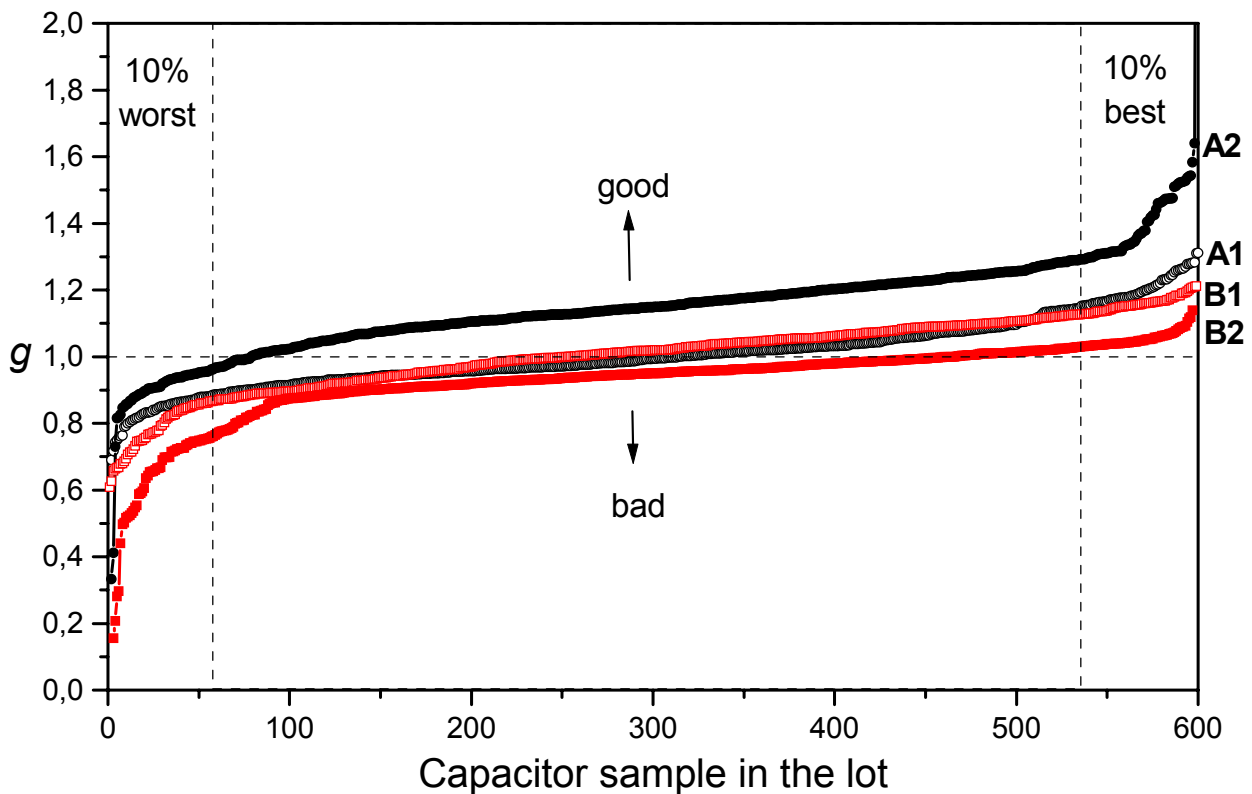


**Fig. 7: Quality quantity  $g$  calculated for various supercapacitor models of two manufactureres (A and B). Reference values are the rated capacitance 1 = 50 F, and 2 = 100 F.**

### 3.7 Thermal aging of capacitance

We investigated comparable supercapacitors of different manufacturers. **Figure 8** shows capacitance determined by the constant current discharge method, divided by the rated capacitance of 50 F printed on the capacitor cases. The discrepancies let us suppose that different methods of capacitance determination seem to be used by the manufacturers.

After three months of storage at an ambient temperature of 90°C and a applied voltage of 2.3 V, capacitance falls dramatically. However, it gets obvious that supercapacitors can be operated under rigorous conditions at least temporarily. The samples of Epcos, Nec/Tokin and Nesscap showed the most stable capacitance in our test. All capacitors fail due to the increasing internal resistance.

The nearby exponential decline of capacitance and the growth of resistance follow the Arrhenius equation. With this, lifetime of the Nec/Tokin supercapacitor can be estimated by roughly 4.6 months (2,5 V) to 7.7 months (2,3 V) and 12.5 month (2.1 V) at 90°C, until the internal resistance quadruples to a value of about 600 mΩ. Lowering operating voltage by 0.4 V stretches lifetime by a factor of about three (2.7).

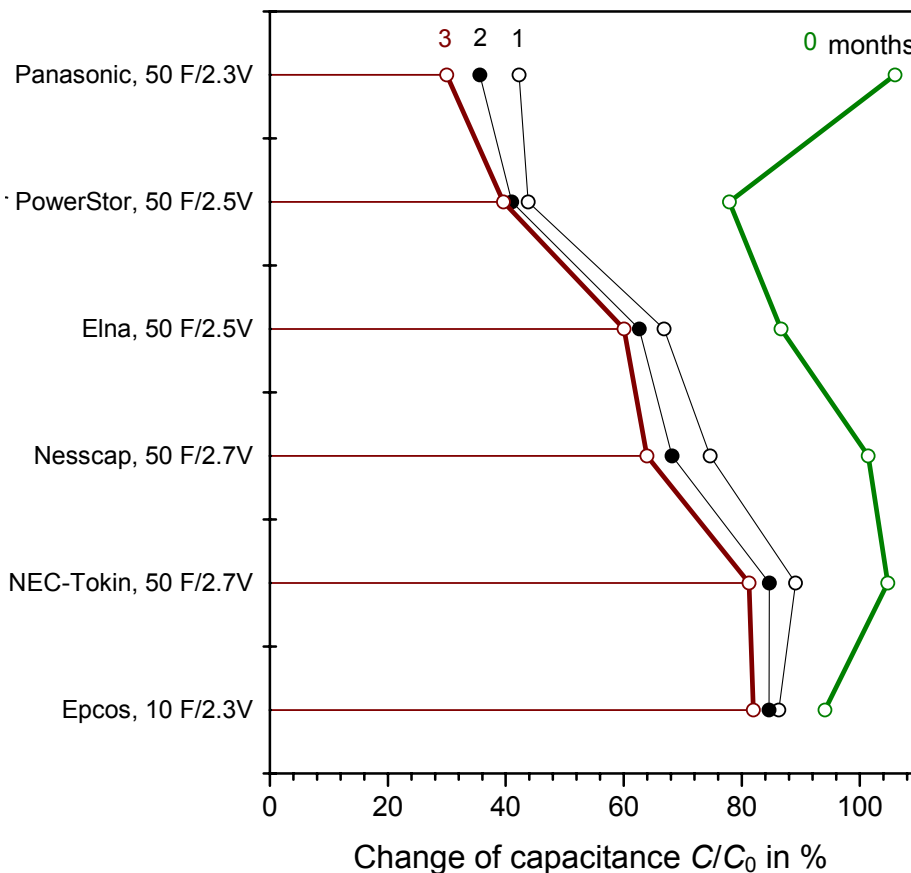


**Fig. 8.:** Aging of commercial supercapacitors. Ratio of measured capacitance and rated capacitance printed on the capacitors cases (0), and decrease of capacitance after one (1), two (2) and three (3) months of storage at 90 °C and 2.3 V.



### 3.8 Chemical aging processes in supercapacitors

The evaluation procedure for statistical lots of supercapacitors shown above can advantageously be used before and after longtime tests.

The nature of the aging process, especially the fact that the impedance spectra before and after a heat treatment (70 °C, 1000 h) are nearly congruent, except a shift of resistance, is outlined in [5]. Double-layer capacitors based on organic electrolytes show a rise of the equivalent series resistance by a factor of 0,5 to 5 during 1000 hours of operation at rated voltage (2.5 V) and elevated ambient temperatures (between 70 and 90 °C). The decrease of capacitance by about 10% is far less affected by heat. The change of resistance seems typical for an “electrical” aging process caused by the growth of isolating interlayers or gas bubbles.

The thermal and electrochemical stability of supercapacitors based on acetonitrile was subject to earlier spectroscopic investigations [7]. Unwanted traces of water in the electroactive materials of supercapacitors play a serious role: In the gas space of commercial supercapacitors, we found excess acetonitrile, water vapor, carbon dioxide and ethene, and fragments of meta boric acid, alkylboron compounds – obviously generated by the hydrolysis and condensation of BF<sub>4</sub> anions. An increasing pressure is built up inside the capacitor by excess acetonitrile, desorbing inert gases, water vapour and decomposition products. Leaky capacitors lose a brownish crystalline mass, which consists of residual electrolyte, organic acids, acetamide, aromatics, and polymer compounds. The alkylammonium cation is destroyed by the elimination of ethene, whereby the catalytical activity of the active carbon electrodes plays an essential role. Acetonitrile forms acetamide, acetic and fluoroacetic acid, depending on the cell voltage and humidity of the electrolyte. The fluoroborate anion is a source of fluoride, hydrogenfluoride and boric acid. In the liquid phase heterocyclic compounds are formed such as pyrazines. The active carbon electrodes lose cyclic siloxanes and aromatic contaminations even at room temperature, and are destroyed mainly at the anode.

### 3.9 Frequency response of ionic liquids

State-of-the-art electrolytes based on acetonitrile and propylene carbonate are limited to a potential window of about 2.5 to 2.7 V. On the other hand, their conductivity of about 100 mS/cm comes close to the best inorganic electrolytes such as sulfuric acid (850 mS/cm) and potassium hydroxide (620 mS/cm). Recently, ionic liquids [16] have been considered as alternative organic solvents.

a) We investigated different ionic liquids with respect to their use in supercapacitors by *ac* impedance spectroscopy using a Solartron “Frequency Response Analyser 1250“ in a frequency range between 10 kHz to 0.1 Hz, a sinewave excitation signal of 1 V, and a 0.1 Ω standard resistor. The measuring cell shown in **Figure 9** comprised two gilt copper stamps (2.5 x 2.5 cm<sup>2</sup>) in a fixed distance of 2 mm. The vacuum capacitance of  $C_0 \approx 3$  pF at 1 kHz was verified by a LCR bridge. The cell constant  $K = R \cdot \kappa \approx 0.027$  cm<sup>-1</sup> was determined by help of 0.1 molar KCl solution ( $\kappa = 0.01215$  S/cm, 22°C) and the measured impedance real part  $R$  at 1 kHz. Capacitance at any circular

frequency  $\omega = 2\pi f$  was calculated from the imaginary part of impedance with reference to a simple R–C series combination.

$$C(\omega) = \varepsilon K = [2\pi f \cdot \text{Im} \underline{Z}(\omega)]^{-1} \quad (11)$$

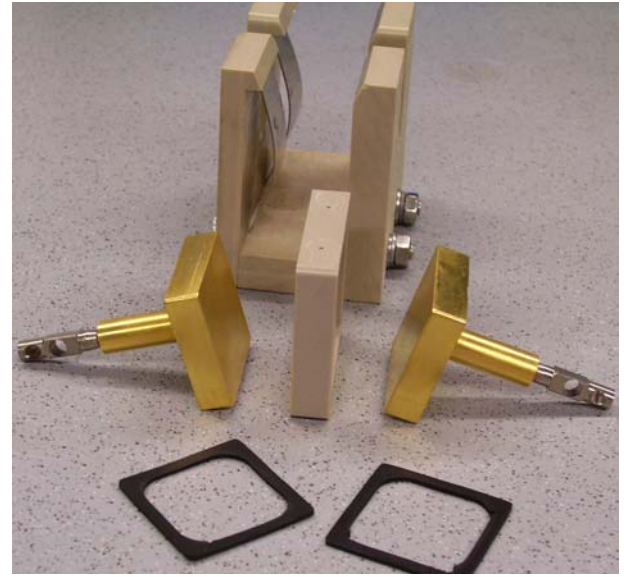
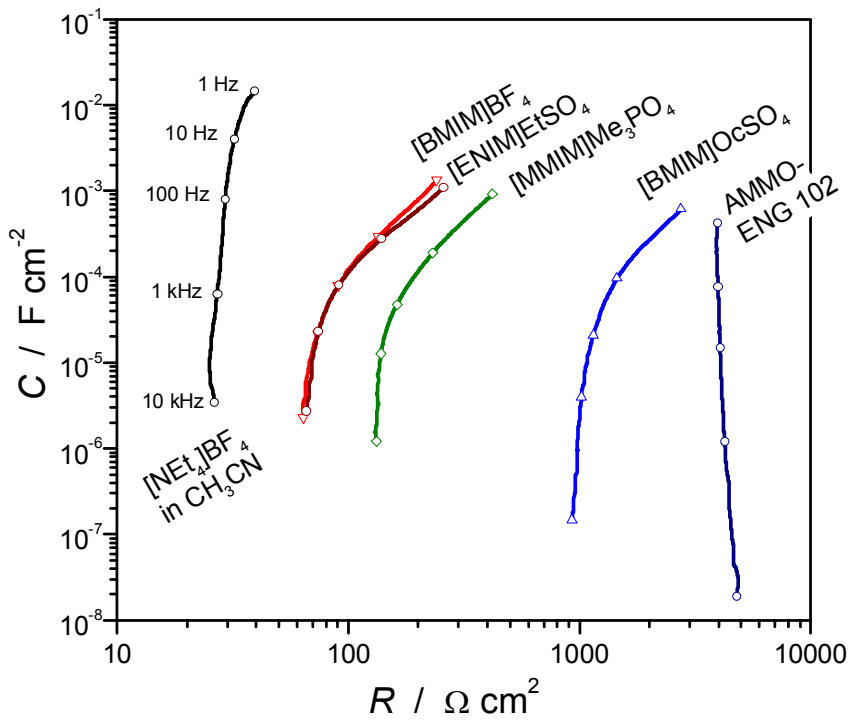
Figure 9 exhibits the low resistance and high capacitance of  $[(\text{C}_2\text{H}_5)_4\text{N}]\text{BF}_4$  in acetonitrile in comparison to novel ionic liquids.

*b)* The temperature dependence of resistance and capacitance was investigated by help of an temperature controlled glass vessel filled with 25 ml of ionic liquid, a glassy carbon working electrode, and a platinum counter electrode. This combination was chosen, because trace amounts of water and protonic impurities in the ionic liquid give rise to small reduction waves in the cyclic voltammogram on platinum but not on glassy carbon. Traces of air and moisture were allowed with respect to the technical applications. The cell constants  $K$  were 0.742 (25°C), 0.790 (40°C), 0.850 (60°C), 0.905 (70°C), 1.204 (85°C), based on literature values for the conductivity of a 1-molar potassium chloride solution,  $\kappa(T) = 0,00193 T/^\circ\text{C} + 0,0634$  (in S/cm), at a frequency of 10 kHz. Conductivity was calculated by help of the real parts of impedance according to  $\kappa(\omega) = K/R(\omega)$ . In all ionic liquids conductivity increased at elevated temperatures, which was to be expected for ionic conductors.

In **Figure 10**, the quantity  $\varepsilon(\omega) = 70 \cdot C(\omega) / 0.77 \text{ mF}$  was calculated as a rough estimate of dissociation and interionic forces. The measured capacitance  $C(\omega)$  was divided by the capacitance of 1-molar KCl solution at 0.5 Hz and multiplied by its permittivity [13], slightly decreasing at higher temperatures.

*c)* Supercapacitor cells built of active carbon electrodes and ionic liquids absorbed by polymer separators did not reveal any advantage compared to  $(\text{C}_2\text{H}_5)_4\text{NBF}_4/\text{acetonitrile}$ . Nevertheless,  $[\text{BMIM}]\text{BF}_4$  and  $[\text{EMIM}]\text{EtSO}_4$  come close. Unfortunately, the ionic liquids in the test showed an unwanted increase of leakage current due to decomposition reactions, and they tend to polymerise at cell voltages around 1,5 to 2 V, especially  $[\text{BMIM}]\text{O}c\text{SO}_4$ , AMMOENG<sup>TM</sup> 102, and  $[\text{MMIM}]\text{Me}_2\text{PO}_4$ . The formation of gas bubbles, white polymer-like strings, and a brownish tinge were observed. The electrolytic and thermal decomposition was therefore not investigated in detail.

Summarizing, organic electrolytes based on acetonitrile show the best conductivity of all solvent systems we have known so far. With respect to the voltage window only,  $[\text{BMIM}]\text{BF}_4$  seems to be a promising substitute of TEABF/acetonitrile. The decomposition voltage equals about 2.5 V at anodic potentials, and about –4 V at cathodic potentials. Unfortunately, ionic liquids tend to decompose and polymerize after several hundred charge/discharge cycles.



2,5 cm x 2,5 cm x 0,2 cm

$K = 0,032 \text{ cm}^{-1}$

**Fig. 9.:** *ac* impedance spectra of ionic liquids in comparison to TEABF<sub>4</sub>/acetonitrile at room temperature. Testing cell with gilt copper electrodes (right). Acronymes see glossary.

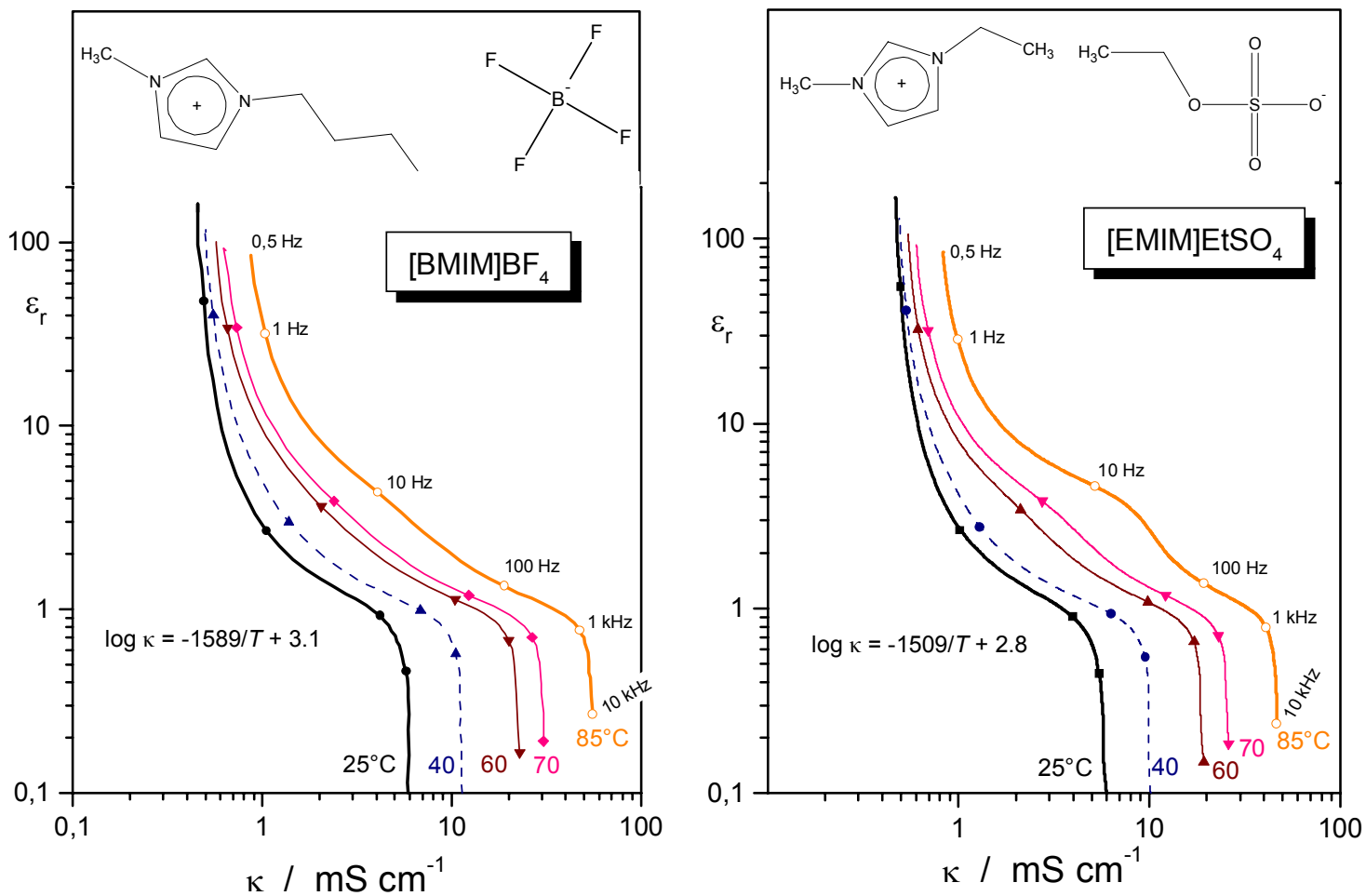


**Figure 10.: Frequency response of ionic liquids at different temperatures: permittivity versus conductivity. In the Arrhenius equation Temperature  $T$  is given in Kelvins.**

## 4. Conclusion and summary

The nature of capacitance is outlined as a dynamic quantity, which depends strongly on the time domain of the applied measuring technique. We were able to gather scaling factors for the conversion of *ac* series impedance capacitances at 1 Hz into values corresponding to *dc* transient techniques: roughly a factor of 1.5 in acetonitrile systems and a factor of 5 in propylencarbonate. The factors refer especially to commercial capacitors in the 100 F range.

A useful quantity for the statistical evaluation of supercapacitor rated data of different manufactureres is presented.

With respect to ionic liquids for supercapacitors, further research is required on highly conductive and chemically inert electrolytes. [BMIM]BF<sub>4</sub> might be a proper candidate to replace TEABF<sub>4</sub>/acetonitrile, although its potential window is 35% more narrow.

## 5. Glossary

[BMIM][BF <sub>4</sub> ]	1-Butyl-3-methyl-imidazolium tetrafluoroborate
[BMIM][OcSO <sub>4</sub> ]	1-Butyl-3-methyl-imidazolium octylsulfate
[MMIM][Me <sub>2</sub> PO <sub>4</sub> ]	1,3-Dimethyl-imidazolium dimethylphosphate
[EMIM][EtSO <sub>4</sub> ]	1-Ethyl-3-methyl-imidazolium ethylsulfate
AMMOENG <sup>TM</sup> 102	N-alkyl-ammonium salt coupled to tallow, manufactured by “Solvent Innovation”, Cologne, Germany

## 6. References

- [1] B. E. Conway, *Electrochemical Supercapacitors*, Kluwer Academic/Plenum Publishers, 1999.
- [2] W. Schmickler (Ed.), *Ladungsspeicherung in der Doppelschicht*, Proc. 2nd Ulm Electrochemical Talks, Universitätsverlag Ulm, 1995, p. 291-310; and literature cited there.
- [3] S. Trasatti, P. Kurzweil, *Platinum Metals Review* **38** (1994) 46-56.
- [4] R. de Levie, Electrochemical response of porous and rough electrodes, in: P. Delahay (Ed.), *Advances in electrochemistry and electrochemical engineering*, Vol. 6, Interscience, New York 1967, p. 329-397.
- [5] P. Kurzweil, B. Frenzel, R. Gallay, Capacitance Characterization Methods and Ageing Behaviour of Supercapacitors *Proc. 15<sup>th</sup> International Seminar On Double Layer Capacitors*, Deerfield Beach, U.S.A., December 5-7, 2005.
- [6] P. Kurzweil, H.-J. Fischle, A new monitoring method for electrochemical aggregates by impedance spectroscopy, *J. Power Sources* **127** (2004) 331–340.
- [7] P. Kurzweil, M. Chwistek, Proc. 10th Ulm Electrochemical Talks (UECT), June 27-28 , 2006, to be published in *J. Power Sources*.

- [8] P. C. Trulove, R. A. Mantz, Electrochemical properties of ionic liquids, in: P. Wasserscheid, T. Welton (Eds.), *Ionic Liquids in Synthesis*, Wiley-VCH, Weinheim
- [9] IEC-40/1378 / DIN IEC 62391-1, Fixed electric double layer capacitors for use in electronic equipment. Part I: Generic specification, June 2004. – IEC-40/1379 / DIN IEC 62391-2, Fixed electric double layer capacitors for use in electronic equipment. Part I: Sectional specification: Electric double layer capacitors for power application, June 2004.
- [10] P. Kurzweil, O. Schmid, A. Löffler, Metal oxide supercapacitor for automotive applications, Replacement of starter batteries. *Proc. 7<sup>th</sup> Int. Seminar on Double Layer Capacitors*, Deerfield Beach, USA, Dec. 8-10, 1997.
- [11] E. Harzfeld, R. Gallay, M. Hahn, R. Kötz, Presentation on Capacitance and series resistance determination in high power ultracapacitors, ESSCAP'04, Belfort, November 2004.
- [12] H. Gualous, R. Gallay, *Technique de l'ingénieur*, D3335, to be published; ESSCAP'04, Belfort, November 2004.
- [13] G. Kortüm, *Lehrbuch der Elektrochemie*, Verlag Chemie, Weinheim 1970, p. 140.

### **Acknowledgement**

The ionic liquids we got thankfully from Prof. Dr.-Ing. A. Jess, University of Bayreuth.

## Figure Captions

Fig. 1: Capacitance of Maxwell capacitors (BCAP0350) determined by different techniques, which cause a different state-of-charge of the capacitor.

Fig. 2: Determination of capacitance using a constant current discharge according to a) IEC 40/1378 and b) the integration method (see text). Maxwell "BCAP0350" supercapacitors (325 F/2.5 V) at different discharge currents of 1 A and 10 A.

Fig. 3: Model for the capacitance of a supercapacitor due to the double-layer  $C_0$  and faradic reactions  $C(U)$ .

Fig. 4: Constant current discharge characteristics of a 30 V/65 F bipolar supercapacitor at different operating voltages  $U$  (states of charge). Capacitance was determined by  $C = I \cdot dU/dt$  at a discharge current of  $I = 11$  A.

Fig. 5: Determination of rated capacitance of a MAXWELL supercapacitor (350 F, 2.5 V) by cyclic voltammetry at different scan rates: a) by the integration method, b) by averaging of differential capacitance  $C(U) = 241 \text{ F} + 85 \text{ U/V}$  at a scan rate of 1 mV/s (fit quality 99,8%).

Fig. 6: Frequency response of capacitance (a) and complex plane plot (b) of supercapacitors of two manufacturers (A, B) rated at 1 = 50 F, and 2 = 100 F.

Fig. 7: Quality quantity  $g$  calculated for various supercapacitor models of two manufacturers (A and B). Reference values are the rated capacitance 1 = 50 F, and 2 = 100 F.

Fig. 8.: Aging of commercial supercapacitors. Ratio of measured capacitance and rated capacitance printed on the capacitors cases (0), and decrease of capacitance after one (1), two (2) and three (3) months of storage at 90 °C and 2.3 V.

Fig. 9.: *ac* impedance spectra of ionic liquids in comparison to TEABF<sub>4</sub>/acetonitrile at room temperature. Testing cell with gold copper electrodes (right). Acronyms see glossary.

Figure 10.: Frequency response of ionic liquids at different temperatures: permittivity versus conductivity. In the Arrhenius equation Temperature  $T$  is given in Kelvins.

Table 1: Rated values of capacitance and series resistance determined by cyclic voltammetry and impedance spectroscopy. The given error equals the experimental standard deviation.